Measurement of a Complete Set of Nuclides, Cross Sections, and Kinetic Energies in Spallation of ^{238}U 1*A* GeV with Protons

P. Armbruster,[1] J. Benlliure,[1,2] M. Bernas,[3] A. Boudard,[4] E. Casarejos,[2] S. Czajkowski,[5] T. Enqvist,[1,*] S. Leray,[4] P. Napolitani,[1,3] J. Pereira,[2] F. Rejmund,[1,3] M.-V. Ricciardi,[1] K.-H. Schmidt,[1] C. Stéphan,[3] J. Taieb,[1,3,†] L. Tassan-Got,[3] and C. Volant[4]

[1]*Gesellschaft für Schwerionenforschung, Planckstraße 1, 64291 Darmstadt, Germany*
[2]*Universidad de Santiago de Compostela, 15706 Santiago de Compostela, Spain*
[3]*Institut de Physique Nucléaire, BP 1, 91406 Orsay Cedex, France*
[4]*DAPNIA/SPhN, CEA/Saclay, 91191 Gif sur Yvette Cedex, France*
[5]*CEN Bordeaux-Gradignan, Le Haut-Vigneau, 33175 Gradignan Cedex, France*

(Received 28 June 2004; published 15 November 2004)

Spallation residues and fission fragments from 1*A* GeV ^{238}U projectiles irradiating a liquid hydrogen target were investigated by using the fragment separator at GSI for magnetic selection of reaction products including ray-tracing, energy-loss and time-of-flight techniques. The longitudinal-momentum spectra of identified fragments were analyzed, and evaporation residues and fission fragments could be separated. For 1385 nuclides, production cross sections down to values of 10 μb with a mean accuracy of 15%, velocities in the uranium rest frame and kinetic energies were determined. In the reaction all elements from uranium to nitrogen were found, each with a large number of isotopes.

DOI: 10.1103/PhysRevLett.93.212701 PACS numbers: 25.40.Sc, 25.85.Ge, 28.41.Kw, 29.25.Rm

In view of the importance of proton-induced spallation reactions in the 1 GeV range for future technological applications and the unique experimental possibilities at GSI [1,2], Darmstadt, a program was initiated to measure isotopic cross sections and kinetic energies. World-wide isotope separators on line (ISOL) have used the proton on ^{238}U reactions for 35 years, and future radioactive-beam facilities producing neutron-rich isotopes count on it, but a solid base for the primary isotopic production is missing. By 1 GeV protons two main reaction channels are populated: spallation evaporation residues (EVR) and fission fragments (FF). In the 1960s Friedlander and collaborators were the first, using radiochemical and surface-ionization techniques, who studied the reactions p + U and p + W at various energies [3]. Isotopes close to the target nuclei and of the alkaline elements rubidium and cesium were identified and measured. In the 1970s systematic measurements on all alkalines were undertaken using on-line mass separators [4,5]. Later investigations of FF in 1 GeV proton reactions on heavy elements using different techniques were performed [6–8]. All results on p-induced fission were evaluated recently [9].

A 1*A* GeV ^{238}U beam from the GSI accelerator facility produced EVR and FF in a liquid H_2-target, 87 mg/cm^2 thick. The target was provided by DAPNIA-Saclay and IPN-Orsay [10]. Fully stripped residues produced in inverse kinematics and emitted into a small cone in forward direction were separated with well controlled efficiencies within 0.3 μs by the high resolution fragment separator (FRS) [1] and its time-of-flight and ΔE detectors. The high resolving power of the FRS enabled the scan of the longitudinal velocity distributions of all isotopes and the analysis of the kinematics of the reactions in the uranium rest frame. For further experimental information, see Refs. [2,11,12]. Based only on physical properties of the radioactive ions, the method does not depend on chemistry. Primary residues are observed, as all β-decay and nearly all α-decay half-lives are longer than the separation times. Finally, cross sections for about 1400 nuclides and their kinetic energies were determined.

In Fig. 1 we present, in a proton-neutron plot, cross sections using a color logarithmic scale. In this unique comprehensive "transmutation" of uranium, all elements from uranium to nitrogen, each with a large number of isotopes, are observed. In the cross-section range down to 10 μb, 1385 nuclides are observed, as shown on the figure. The total cross section of (1.97 $\pm$ 0.3) b divides

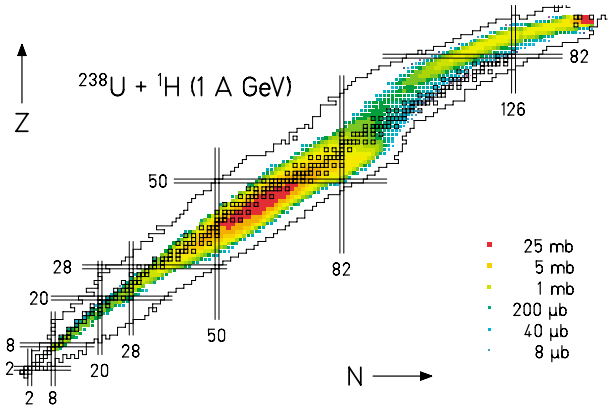

FIG. 1 (color). The identified nuclides are shown on a chart of nuclei. Numerical values are available on http://www-w2k.gsi.de/kschmidt/data.htm. The experimental cross sections are indicated by a logarithmic color scale.

in (1.53 ± 0.2) b for fission [12] and (0.44 ± 0.1) for EVR [11]. It is of primary interest to understand the large fraction (78%) observed for nuclear fission. For elements beyond tungsten, $Z > 74$, EVR dominate over fission fragments [11], whereas FF identified by their kinematics of a binary break-up process populate all the range below tungsten down to the lightest element observed, nitrogen. Data on fission fragments are published for $Z = 28$ to 63 [12]. The missing lightest and the heaviest elements, $Z =$ 7–31 [13] and $Z = 64$–74 [14], respectively, accomplish the full distribution which is presented as a highlight of this Letter.

Figures 2(a) and 2(b) show integrated distributions of cross sections depending on atomic and neutron numbers. EVR and FF merge in the minima at $Z = 71$ and $N = 97$ (^{168}Lu).

The Z distribution of EVR, Fig. 2(a), decreases steadily going to lighter elements down to $Z = 74$. A shoulder is seen in the range $Z = 80$ to 88 corresponding to the wide plateau seen in the N distribution to be discussed below.

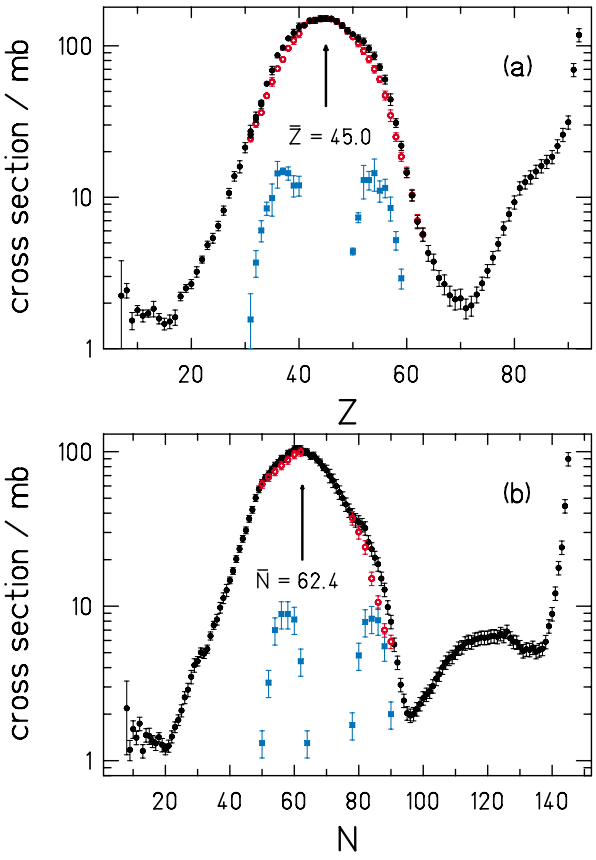

FIG. 2 (color). a) Measured Z distribution for all elements between $Z = 7$ and 92; b) Measured N distribution for all neutron numbers between $N = 8$ and 146. Summed cross sections (full point) from cross sections for low-energy asymmetric fission (blue squares) and for high-energy symmetric fission (red empty points) are reported separately. The minima at $Z =$ 71 and $N = 97$ separate EVR and FF.

The distributions of FF reveal a small 5% contribution of the classical asymmetric low-energy fission [12]. The underlying parent nuclei are relatively cold. They cluster around ^{233}U but may reach down to $A_0 = 226$ [15]. Having separated this asymmetric contribution from the total Z distribution, a mean atomic number of $Z = 44.9$ is found. The remaining distribution is surprisingly symmetric and has a standard deviation of 6.4 charge units. A contribution from lighter fissioning parent nuclei, which should increase the cross section of the lighter part of the distribution, is barely visible in the range $Z = 20$ to 30. At very large mass asymmetries of the FF, $Z_1/Z_2 < 20/70$, the cross sections pass a minimum and increase slightly for most extreme asymmetries. This was seen before [16] and is explained by the Businaro-Gallone mountain [17] in the liquid-drop potential energy surface (LDM-PES).

The N distribution of EVR, Fig. 2(b), shows an extended plateau between $N = 138$ and $N = 110$ at a low level of 5.0 to 6.4 mb which specifies highly fissile parent nuclei ($Z_0^2/A_0 > 34$). These small cross sections are observed for spherical nuclei around $N = 126$, having large ground-state shell-corrections and thus also increased fission barriers. At the excitation energies of the fissioning parent nuclei produced in our reaction, the higher barriers give no increased survival against fission. The enhanced fission probabilities at $N = 126$ are explained by the low level densities for nuclei with spherical ground states [18]. Small sections are observed as well for highly fissionable nuclei, being deformed and having much smaller ground-state shell-corrections at the upper limit $N = 138$ of the plateau. They are found even down at the lower limit, $N =$ 110, in the region of $Z = 80$ to 82. Finally, in the range of $N = 110$ to 100, cross sections break down. At 1A GeV the excitation energy transferred in the reaction approaches its upper limit at about 500 MeV for mass losses of $\Delta A > 50$.

The$N$ distribution of FF, Fig. 2(b), has a mean value of $N = 62.4$. The low-energy asymmetric fission subtracted, we obtain the high-energy symmetric distribution with a mean neutron number of 61.9. Combined with the mean proton number 44.9 obtained from the Z distribution, a mean mass number of $A = 106.8$ is reconstructed for FF. ^{107}Rh is the mean nuclide produced in high-energy symmetric fission. A small surplus of cross sections at $N =$ (30 ± 6) may indicate fission from lighter parent nuclei down in the range of $Z_0 = 80 \pm 4$. These could be the asymmetric fragments of the tail of the symmetric fission channel, originating from fissioning parent nuclei located at the lower limit in the plateau and in its fall.

The measured standard deviation of the high-energy symmetric Z distribution, Fig. 2(a), of $\sigma_Z = 6.4$ a.u. is related via the curvature of the LDM-PES to the excitation energy of the mean parent nucleus at the fission barrier [19–21]. With a fission barrier of 4 MeV, an energy above ground state of (58 ± 10) MeV is obtained, allow-

ing for an emission of six neutrons. Adding these neutrons emitted from the fragments to the neutron number of the mean pair of fragments, (2×61.9), a neutron number of $N_0 = (130 \pm 1)$ follows for the mean parent nucleus. For high-energy symmetric fission, ^{220}Th is the mean parent nucleus reconstructed from the isotopic distribution of FF.

For the complete set of FF produced in the reaction, we obtain for each element the mean neutron-to-proton ratio $\overline{N}/Z$ and the width of its isotopic distribution $\sigma_N^{Z=\text{const}}$. These values are shown in Figs. 3(a) and 3(b) separated into low-energy asymmetric and high-energy symmetric fission. They describe the isospin dependences of the cross sections. The $\overline{N}/Z$ ratio of the mean fission fragment ^{107}Rh, 1.38, is found to be smaller than for low-energy fission where $\overline{N}/Z = 1.53$.

Figure 3(a) shows in the range $Z = 34$ to 56, increasing $\overline{N}/Z$ ratios for high-energy symmetric fission. The slope observed agrees with a charge polarization expected for a smooth LDM-PES showing no nuclear structure effects [22]. A new finding is the rapid decrease of the mean

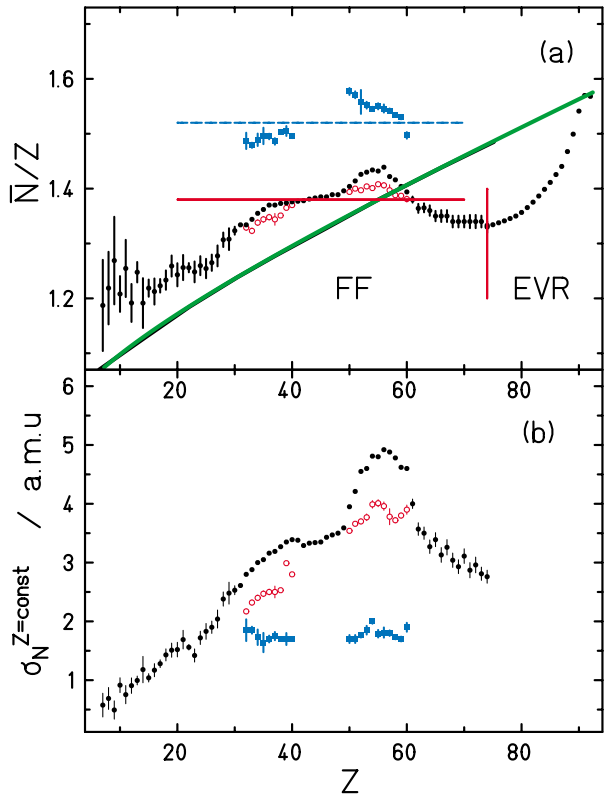

FIG. 3 (color). a) The mean $\overline{N}/Z$ ratio and b) the standard deviation $\sigma_N^{Z=\text{const}}$ are plotted as function of the atomic number. Symbols present the different contributions (see Fig. 2). The valley of stability (green line) is shown. The mean $\overline{N}/Z$ ratio for the low-energy asymmetric process (dashed blue line) and for ^{107}Rh representative of the high-energy process (red line) are indicated. The vertical line at $Z = 74$ separates fission fragments from spallation residues.

neutron density for isotopes at higher asymmetries. Taking as the mean parent nucleus ^{220}Th and as the most asymmetric pair observed, $Z_1/Z_2 = 16/74$, mean neutron numbers $N_1/N_2 = 19/99$ are reached adding up to 118 neutrons present in the FF. Twelve neutrons are lost indicating a high excitation energy of about 100 MeV. This energy is distributed in the high-energy regime between the pair of FF proportionally to their masses. The heaviest elements lose up to ten neutrons, and beyond erbium, $Z > 68$, all isotopes observed are stable or proton-rich. Neutron-rich isotopes in the wings of the Z distribution will come with very low cross sections for the higher elements. It is the small contribution of low-energy asymmetric fission of (105 ± 10) mb which stays the main source of neutron-rich isotopes for elements in the range $Z = 28$–64 [23].

The standard deviation $\sigma_N^{Z=\text{const}}$ of the isotopic distribution for a given element is presented in Fig. 3(b). The mean value of $\sigma_N^{Z=\text{const}} = (3.3 \pm 0.2)$ a.u. taken over the range $Z < 74$ compares well to $\sigma_N^{Z=\text{const}} = (3.2 \pm 0.7)$ a.u. measured in ^{238}U 0.75A GeV on ^{208}Pb [24]. For asymmetric low-energy fission, $\sigma_N^{Z=\text{const}} = (1.8 \pm 0.2)$ a.u. agrees with $\sigma_N^{Z=\text{const}} = (1.7 \pm 0.05)$ a.u. from ^{238}U 0.75A GeV on ^{208}Pb [25]. High-energy symmetric fission shows a mean standard deviation wider by a factor 1.8 compared to asymmetric low-energy fission. The ratio of standard deviations for the two fission mechanisms decreases from 2.2 for barium ($Z = 56$) to values close to 1 for the lighter elements. This trend to a larger width of the isotopic distributions going to heavier elements reflects the widening of the LDM-PES in the (N-Z) degree of freedom and the extended range of isotopes contributing to fission. As observed for the $\overline{N}/Z$ ratio, $\sigma_N^{Z=\text{const}}$ decreases for $Z > 56$. The shift to smaller values for elements between $Z = 58$–74 is also visible in Fig. 1 showing the long plane of low cross sections colored in green.

Figures 4(a) and 4(b) show the mean velocities of FF in the uranium rest frame and kinetic energies for the elements produced as EVR or FF. A comparison with calculated velocities of FF, Fig. 4(a), indicates that a small number of elements in the range $Z_0 = (88$–$92)$ dominates the family of parent nuclei. The systematic measurement of kinetic energies of spallation EVR, Fig. 4(b), is a primer achieved by our experimental method. Their kinetic energies are very small, on the average about 2.9 MeV. In this energy range slowing down of heavy ions mainly proceeds by elastic collisions. The maximum of kinetic energies at one third of the atomic number of the parent nucleus, as expected for symmetric fission of a monoisotopic fission source, is experimentally verified.

The complete data set presented is a main step forward, which in this Letter stands for itself. Certainly our work is not finished here. The tasks to be done in the near future are open: 1) The energy dependence of the cross

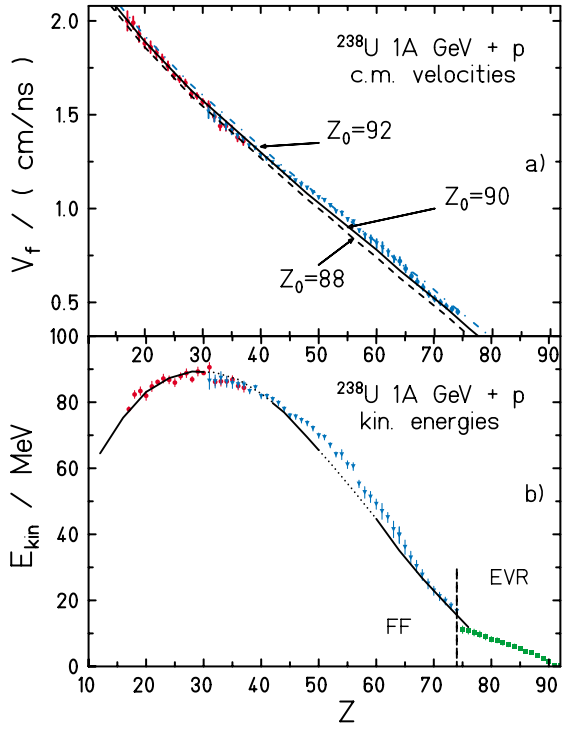

FIG. 4 (color). a) The mean c.m. velocity of fission fragments measured as a function of the atomic number. The three lines: dashed line ($Z_0 = 88$), full line ($Z_0 = 90$), and dashed-dotted line ($Z_0 = 92$), are calculated assuming Coulomb repulsion with a radius constant r_0 being kept constant and fixed by the measured value of the velocity for symmetric fission of ^{220}Th taken as normalization. The blue triangles and the red points refer to Ref. [12] and to Ref. [13], respectively. b) The mean kinetic energies of the elements as a function of the atomic number, symbols as above and green squares from Ref. [11]. The full line is a calculation for ^{220}Th using the conditions as in the legend above. Asymmetric fission contributes in the regions indicated by the dotted lines.

sections is hardly known. Further measurements at lower energies are needed for our reaction. 2) Our data should serve as a bench mark for simulation codes of the complex physics of spallation reactions with the final goal to predict unknown systems. 3) An innovative measuring technique giving more and more precise and complete results generates a better understanding of the underlying physics. Further contributions to fundamental aspects of spallation reactions may still emerge in a coming analysis.

Financial support by EU Contract No. ERBCHBCT940717 for J. B., T. E., and F. R. and by GSI for P. N., M. V. R., and J. T. is gratefully acknowledged. This work was partially supported by the European Union in the HINDAS project (Contract No. FIKW-CT-2000-00031) and by the project Access to Large Facilities (Contract No. EC-HPRI-CT-1999-00001).

*Present address: CUPP-project P. O. Box 22 FIN-86801 Pyhäsalmi, Finland
†Present address: CEA/Saclay DM2S/SERMA/LENR, 91191 Gif/Yvette CEDEX, France

[1] H. Geissel *et al.*, Nucl. Instrum. Methods Phys. Res., Sect. B **70**, 286 (1992).
[2] T. Enqvist *et al.*, Nucl. Phys. **A686**, 481 (2001).
[3] G. Friedlander *et al.*, Phys. Rev. **129**, 1809 (1963).
[4] R. Klapisch *et al.*, Nucl. Instrum. Methods **53**, 216 (1967).
[5] B. N. Belyaev *et al.*, Nucl. Phys. **A348**, 479 (1980).
[6] B. A. Bochagov *et al.*, Sov. J. Nucl. Phys. **28(2)**, 91 (1978).
[7] L. A. Vaishnene *et al.*, Z. Phys. A **302**, 143 (1981).
[8] Yu. Titarenko *et al.*, Nucl. Instrum. Methods Phys. Res., Sect. A **414**, 73 (1998).
[9] A. V. Prokofiev, Nucl. Instrum. Methods Phys. Res., Sect. B **463**, 557 (2001).
[10] P. Chesny *et al.*, in GSI Annual Report, 1996, Vol. 1997-1, p. 190.
[11] J. Taieb *et al.*, Nucl. Phys. **A724**, 413 (2003).
[12] M. Bernas *et al.*, Nucl. Phys. **A725**, 213 (2003).
[13] V. Ricciardi (to be published).
[14] M. Bernas *et al.* (to be published).
[15] K.-H. Schmidt *et al.*, Nucl. Phys. **A665**, 221 (2000).
[16] D. G. Sarantites *et al.*, Phys. Lett. B **218**, 427 (1989).
[17] U. Businaro and S. Gallone, Nuovo Cimento **1**, 1277 (1955).
[18] A. R. Junghans *et al.*, Nucl. Phys. **A629**, 635 (1998).
[19] A. Ya. Rusanov *et al.*, Phys. At. Nucl. **60**, 683 (1997).
[20] S. I. Mulgin *et al.*, Nucl. Phys. **A640**, 375 (1998).
[21] J. Benlliure *et al.*, Nucl. Phys. **A700**, 469 (2002).
[22] P. Armbruster *et al.*, Nucl. Phys. **A140**, 385 (1970).
[23] M. Bernas *et al.*, Phys. Lett. B **415**, 111 (1997).
[24] W. Schwab *et al.*, Eur. Phys. J. A **A2**, 179 (1998).
[25] C. Donzaud *et al.*, Eur. Phys. J. A **A1**, 407 (1998).